IEPC 2003-62

30mN-CLASS MICROWAVE DISCHARGE ION THRUSTER

Kazutaka Nishiyama, Hitoshi Kuninaka, Yukio Shimizu , Kyoichiro Toki
Institute of Space and Astronautical Science
3-1-1, Yoshinodai, Sagamihara, Kanagawa 229-8510, Japan
(E-mail : nishiyama@ep.isas.ac.jp)

Abstract

This paper presents the development status of a 20-cm diam. microwave discharge ion thruster which generates 25~30 mN of thrust with an electric power of 1kW. By optimizing the discharge chamber length, magnetic field and propellant flow injection, ion currents of up to 530 mA at a net microwave power of 100 W were obtained. We now concentrate upon improvements of microwave launching devices which are lighter, more compact and capable of higher power transmission. Almost the same performance has been achieved with a new launcher, which removes the need for a long circular waveguide. By controlling the microwave frequency, the microwave reflection can now be eliminated almost totally. A higher frequency and stronger magnets have been tested for performance improvement and turned out to be very promising.

1. Introduction

The Institute of Space and Astronautical Science (ISAS) has been developing an ion engine system (IES) for the MUSES-C asteroid sample return mission which employs four μ10 (myu-ten) ion thrusters [1]. The MUSES-C/IES has introduces an original concept in terms of its plasma production method; Electron Cyclotron Resonance (ECR) discharge induced by microwave injection into discharge chambers of both the ion source and the neutralizer. In parallel to the successful flight model development and integration to the spacecraft, there are a number of future missions employing that technology, such as sample return from several asteroids by only one deep space probe, formation flight of several satellites for space telescope missions, Jupiter probe [2], escape from the ecliptic plane after Jupiter swing-by, and so on, all of which are presently undergoing active discussion and scrutiny by Japanese space scientists and engineers.

In order to implement these challenging missions by using the relatively small launchers available in Japan, electric propulsion systems that are more powerful than MUSES-C/IES may sometimes be required. Japan has three ion propulsion systems; ISAS/NEC μ10 thruster (microwave discharge type, 10 cm, 7 mN, 2700 s), NASDA/MELCO (Kaufman type, 13 cm, 23 mN, 2500 s) [3] and NAL/TOSHIBA (Ring cusp type, 35 cm, 150 mN, 3500 s) [4]. ISAS has just started the serialization of its microwave discharge ion thruster, being referred as the "μ" series named after its "M" series solid propellant spacecraft launchers in order to fill the gap in the 30-90 mN thrust range, which cannot be easily covered by throttling the 150 mN thruster previously mentioned. At first, laboratory models of 20-cm diam. thruster have been designed and tested with tentative goals as summarized in Table 1.

The new 20-cm ion thruster μ20 will have four times larger beam area than that of the μ10, will generate four times larger thrust, and will do so more efficiently. The chosen microwave frequency is identical to that adopted for the μ10, based on considerations of the dependency of microwave launcher performance on frequency as well as the difficulty and amount of time required to assess and tune the thruster performance at various different frequencies. Ion optics will involve the usage of a carbon-based 3-grid system with a higher elastic modulus than μ10's. The first ion optics fabricated for the μ20 are shown in Fig. 1, with a grid thickness of 1.0 mm for all cases. Further improvement is necessary in order to achieve thinner and mechanically stronger grids. More details on ion optics can be found in references [5] and [6].

As for the neutralizer, its size will not be different from that of μ10 neutralizer. In the initial tests, an electron emission current of 600 mA necessary for the μ20 was obtained at an expense of a microwave power of 25 W and a xenon flow rate of 1 SCCM. The coupling voltage was about 30 V, which is sufficiently low to achieve the same 18,000h lifetime level as for the μ10.

In this paper, the evolution of the discharge chamber configuration and its performance are described.

2. Ion Source Design Considerations

An ECR discharge was first applied to a 30-cm plasma generator for ion propulsion by H. Goede at the TRW Space and Technology Group in the late 1980's [7]. A few years after, this research was ceased, and we at the ISAS electric propulsion section started work on a 10-cm ion thruster using the same plasma discharge mechanism. Goede introduced the advantages of having an azimuthal cusp (so called ring-cusp) magnetic field arrangement, in contrast to the axial-line cusp. Accordingly, we followed his proposal and designed initial laboratory models just by scaling down his device. However, it turned out that the ring-cusp configuration in a bucket-like discharge chamber with large volume [8] was not suitable for a 10-cm plasma generator, and it was found during development process of μ10 by ISAS [9] that a magnet system with a pair of magnet lines inclined to the plasma source exit and a much shorter chamber length [10] yields higher performance. Incidentally, the μ10 ion source has a very short plasma chamber in which the ion optics is located very close to the ECR region corresponding to a magnetic field strength of 0.15 T [11]. In the course of developing the μ20 ion source, we have considered several chamber designs as illustrated in Fig. 2.

2.1 Permanent Magnet Layouts and Discharge Chamber Geometries for the μ20 Ion Source

We started tests with a plasma generator design which had only one continuous ring plasma region between two magnet rings, surrounding a waveguide exit hall located at the center of the discharge chamber (μ20-I in Fig. 2). This design was considered the most simple scaling-up from the μ10. The second design (μ20-II) is a concept similar to TRW's 30-cm source, in an attempt to promote plasma diffusion into the central and field-free region with a large volume from the ECR region in the vicinity of magnet faces. In the third design, the distance between the magnet lines is basically similar to the distance value for the μ10, and the chamber length is shorter than the former two design concepts. The only salient difference is the most inner magnet lines, where the distance to the neighboring magnet line is twice the distance for others; this way, microwave propagation to the outer ECR regions is not disturbed by the production of a plasma being too dense around the inner ECR regions.

All the configurations have flexibility in their axial length by replacing the side-wall cylinder, as a small variation in axial length affects to the thruster performance. Because the ECR plasma is tightly confined in the *banana-shaped* region between the magnetic field cusps, the ion optics positioned far from the ECR region cannot extract the produced ions efficiently. If the ion optics are located too close to the ECR region, the plasma production volume decreases due to obscuration by a screen grid and electrons that pass through the ECR zone more than once may be lost to the grid surface, resulting in an increase in the ion production cost. Thus, the discharge chamber axial length is one of the main design parameters in thruster concepts other than the μ20-II.

2.2 Microwave Launching Methods

The first three concepts utilize a coaxial-line to circular-waveguide transducer, which is inherited from μ10 ion thruster. Original laboratory models of the μ10 employed a waveguide-based microwave transmission system, as is typical in ground applications of ECR plasma sources. Since building the entire microwave circuit using waveguides is impossible due to the weight penalty it imposes, a microwave amplifier output is connected to the ion source via coaxial cables in case of space applications. Although this microwave launcher is sufficiently optimized and its optimization process is well established, its overall length being too long and its relatively large weight recommend switching to a better microwave launching method.

The μ20-IV shown in Fig. 2 employs a microwave excitation probe (or antenna) at the center of the discharge chamber. The magnet system is identical to that of the μ20-III. This direct probe insertion has been employed in our neutralizer by using an SMA type connector [5]. Considering that, as an ion source the microwave power input is much larger than that of the neutralizer, high power connectors are desirable, such as N- and TNC-type. Experiments were conducted using commercial N-type panel receptacles in combination with various extensions for the center conductor acting as an antenna and an outer conductor that can adapt receptacles to the same discharge chamber as the μ20-III. It must be said that employing the waveguide originally designed for the μ10, with has an inner diameter of 45 mm, would result in a waste of the precious plasma production volume in the center region of the μ20 chamber. The new microwave launcher should help increase the thrust generated with the same chamber diameter due to its compactness.

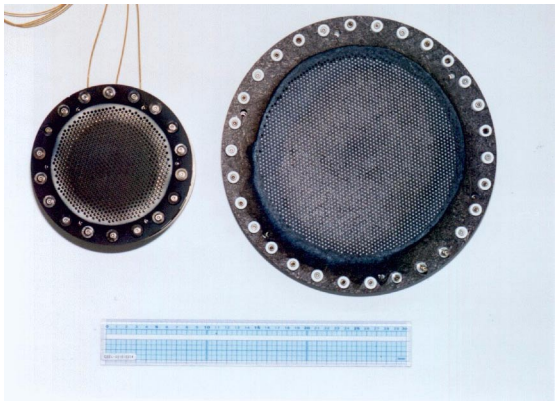

Fig. 1 Carbon/Carbon composite grid assemblies for the μ10 thruster (left) and μ20 thruster (right).

Table 1 Target Performance of 20-cm-diam Thruster

	μ10	μ20
Thruster Size (Beam Area)	ϕ10 cm	ϕ20 cm
Beam Voltage (V)	1500	1200
Beam Current (mA)	140	580
Microwave Frequency (GHz)	4.25	4.25
Microwave Power For Ion Source (W)	32	90
Microwave Power For Neutralizer (W)	8	18
Xe Flow Rate (SCCM)	2.9	11.2
Thrust (mN)	8.1	30.4
Isp (s)	2910	3100
Propellant Utilization (%)	83	80
Ion Production Cost (W/A)	220	155
Total Power (W)	390	1015
Thrust/Power (mN/kW)	20.3	30
PPU Input Power (W)	262	770
PPU Efficiency (%)	80	90
MPA Input Power (W)	99.9	196
MPA Efficiency (%)	55	55

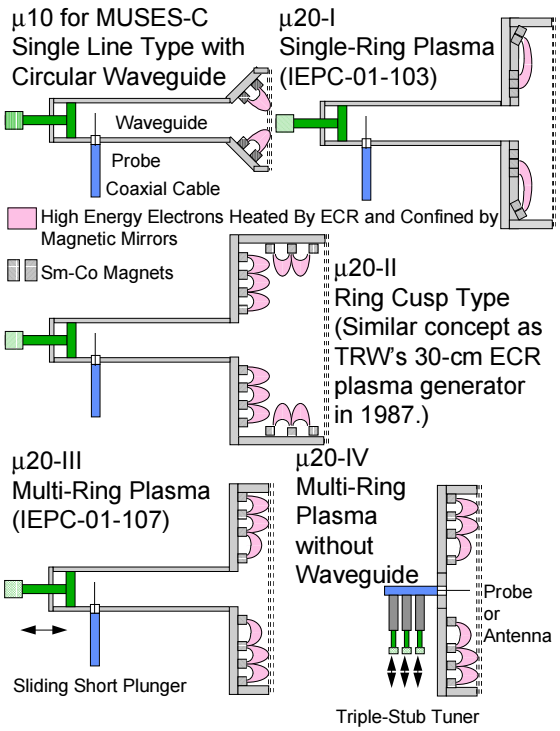

Fig. 2 Discharge chamber geometries considered as candidates for the 20-cm diam. ion thruster μ20.

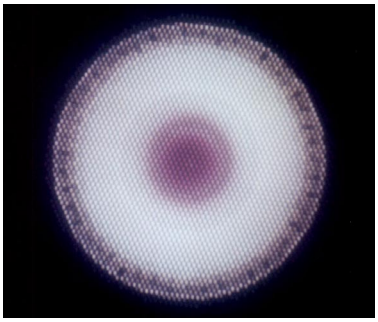

Fig. 3 Plasma discharge of the μ20-I under beam extraction at a microwave power of 48 W. A beam current of 210 mA was obtained at 4.4 SCCM.

3. Summary of Experimental Results of Old Types of μ20 Thrusters

At present, thruster operation employing ion optics has been carried out only for the μ20-I and μ20-III configurations. Conversely, the ion current was collected by a gridded stainless-steel plate biased at -30 V relative to the grounded discharge chamber for the μ20-II, III and IV configurations. This simulated thruster operation simplified experimental hardware, including various chamber lengths, magnet layouts, and different types of microwave launchers. In the case of the microwave discharge ion thruster, the plasma generator design dominates the overall thruster performance and optics tuning should be preceded by chamber optimization. For comparison of ion extraction by the ion collector and by the ion optics in the near future, a discharge pressure inside the plasma generator of approximately 2×10^{-4} Torr (nitrogen equivalent pressure measured by an ionization gauge) was established by supplying 6 SCCM of xenon flow, which is usually the optimum discharge pressure under beam extraction condition for ECR discharge in these devices in order to achieve highest thruster performance.

3.1 Single-Ring Plasma Type (μ20-I)

As reported in Ref. 5 this discharge chamber had an excellent self-ignition capability by microwave insertion. With a microwave power of 30 W, the ECR discharge was ignited and could be sustained with just

10 W. Plasma luminosity, shown in Fig. 3 was very uniform and the discharge was stable. Ion beam acceleration was conducted using the C/C based optics and 10-12 mN thrust was generated at a net microwave power of 40 W. Although the thruster performance at the low power range was not so poor, the thrust was lower than the target value. The low plasma density may be caused by the inefficient electron cyclotron heating with longer distance between magnetic cusps than that of μ10 and by the poor plasma confinement with the cusped magnetic field, due to the small mirror ratio generated by too large a magnet width. This chamber design concept cannot be applied to a larger 30-cm plasma generator, to be developed in the future, due to the non-existence of magnets stronger than SmCo magnets. Considering this argument, further improvements to this chamber were stopped, although there is a possible modification plan about chamber length and waveguide design to reduce microwave reflection.

3.2 Ring-Cusp Type (μ20-II)

As for the μ20-II discharge chamber with a large field free region, the plasma discharge was started by drawing electrons emitted from a filament cathode outside the discharge chamber by applying a voltage of -100 V to the cathode. The ECR plasma was confined around the ECR region and no diffusion to the chamber center was observed. The extracted ion current was extremely low. A larger microwave power up to 180 W was introduced, aiming to induce a discharge mode shift from the ECR region to the field free region found in the TRW plasma generator. However, such shift did not take place and the microwave probe was severely eroded due to a breakdown between inner and outer conductors caused by a strong standing wave generated in the waveguide. Consequently, we have learned that this chamber configuration is not useful for adoption in a 20-cm class ion source, and that the microwave probe used in the μ10 thruster cannot be applied reliably to high power applications over 150 W.

3.3 Multiple Magnet Lines Type (μ20-III)

This discharge chamber with a flat yoke with many thin and concentric grooves permitted the construction of various magnet layouts [12]. Production of a number of concentric plasma rings by microwave launching from the center of the discharge chamber poses a number of possible problems involving plasma uniformity and discharge stability. Mode hopping between several plasma density distributions may sometimes occur, particularly in discharge chambers larger than that of the μ10 thruster, in which more than one microwave E-field modes exist. Concerning the elimination of the discharge mode instability, several configurations shown in Fig. 4 were tested in order to reduce the number of plasma discharge region isolated in a radial direction by connecting the inner and outer magnet rings. All the configurations showed the best performance with an axial chamber length of 30 mm. Concerning the μ20-III discharge chamber, microwave reflection was kept lower than 30 W in many cases by changing a sliding short plunger position with a maximum microwave forward power of 200 W. Net microwave power was calculated by taking the reflected power and cable loss into account.

The magnet arrangement tested first is illustrated in Fig. 4-a). This has two magnet bridges in the radial directions so that high energy electrons can fly between inner and outer discharge regions by $\boldsymbol{E}\times\boldsymbol{B}$ drift or grad B ($\boldsymbol{B}\times\nabla B$) drift. With this magnet arrangement, two crescent shaped plasma rings were produced at the same time and an ion current of 345 mA were collected with the punching metal for ion extraction at a net microwave power of 100 W.

A fully continuous plasma filling a larger volume in the chamber was generated in the second arrangement shown in Fig. 4-b), and a larger ion current of 410 mA was obtained at a lower microwave power of 80 W. Although the plasma production capability was improved relative to the former magnet arrangement, the discharge became unstable at microwave powers larger than 80 W, probably due to the asymmetry of the plasma shape. A 35-mm long discharge chamber with ion optics, which is 5 mm longer than what usually employed in ion collection experiments, generated an ion beam current of 450 mA at a xenon flow rate of 9.3 SCCM and at a microwave power of 80 W. Judging from the fact that discharge chambers longer than 30 mm always give lower collected ion currents, the C/C optics can extract at least a 10 % greater amount of ion beam current than what may be collected by the 30 V negatively biased punching metal.

The best performance and most stable operation so far was achieved by the magnet system illustrated in Fig. 4-c), after a number of trial-and-error tested involving the magnet arrangement which are not described herein. A picture of the plasma luminosity is shown in Fig. 5. This configuration has a center ring part around the waveguide exit and two crescent shape parts outside. An ion current of 480 mA was extracted at a net microwave power of 100W. The reflected power was lower than 5 % of the forwarding power.

By adding four gas ports on the side wall to the original two ports beside the waveguide (Fig. 4-d)), a slight performance improvement was observed. By optimizing the gas flow distribution between the ports, the maximum ion current was increased to 500 mA by introducing a microwave power of 130 W [12].

3.4 Multiple Magnet Lines Type with a Microwave Excitation Probe with a Triple Stub Tuner (μ20-IV)

Indeed, at a first sight re-using the same probe as the one employed in the waveguide type launcher would be a "shortcut" approach. However, its power capacity seems to be about 150 W under the presence of a strong standing wave. In order to develop future higher power thrusters such as the envisaged μ30, a completely new design in which a larger gap between the inner and outer conductors is secured will be necessary. Prototypes of the new compact microwave launcher were fabricated by modifying commercially available N panel receptacles.

The probe design involves quite a large number of parameters such as;

- Center conductor and outer conductor diameters.
- Type of dielectric material facing the discharge chamber.
- Width of the gap between the center conductor end and the screen grid that determines the capacitance at that particular location, which is of paramount importance in terms of impedance matching for effective microwave power absorption to the ECR plasma.
- Geometry of the center conductor.

Since there are no sufficient theoretical design guidelines available, we had to develop them by a trial-and-error approach. Photographs shown in Fig. 6 and Fig. 7 were taken during the course of experiments using the first tested piece, but without a triple stub tuner for impedance matching. The first figure concerns a geometry with concentric magnet lines, and the second one is for the same magnet system as shown in Fig. 4-c). As expected, the concentric arrangement yields a partially luminous plasma and large microwave power reflection. On the other hand, the unique magnet arrangement proposed in the μ20-III configuration produces an uniform discharge plasma again in combination with the microwave excitation probe. When a microwave power of 120 W was applied to the transmission line, only 4 W were reflected to the power supply, without usage of any impedance matching components.

After modifying the probe, we attained good performance, reaching values very close to the highest ones obtained with waveguide type μ20-III. Performance comparison between μ20-III and μ20-IV with a triple stub tuner is shown in Fig. 8. The maximum ion current reached 470 mA at a net microwave power of 120 W.

The microwave probe still had a serious problem involving the dielectric PTFE surface erosion and its short lifetime. Considering this, we switched back to the commercial probe which had been used in the μ10 and μ20-III by covering its surface with a small cap made of BN which in fact extends the operating power range. This version of the discharge chamber is called μ20-V and will be described in the section 5.

The μ20-III has a dead volume without plasma production at the chamber center and its diameter is as large as 70 mm. In order to investigate effect of increasing plasma production volume at the central region, another magnet ring was added just around the microwave probe launcher. As shown in Fig. 9, this resulted in performance degradation, due to the generation of a dense plasma around the probe as well as the poor electron heating in outer region due to microwave E-field attenuation.

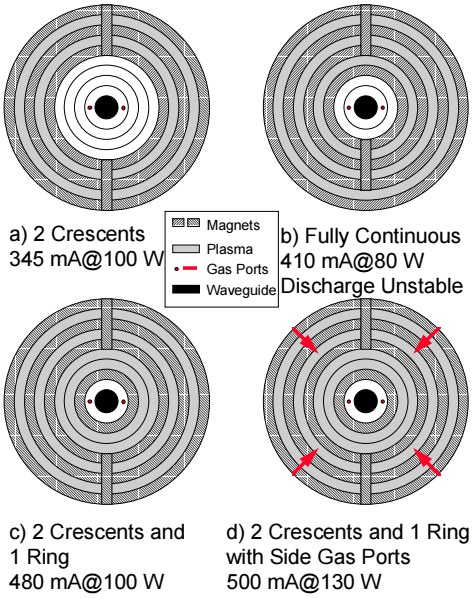

Fig. 4 Various magnet arrangements and gas injection methods tested with the μ20-III thruster.

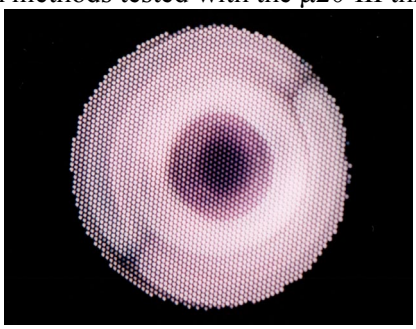

Fig. 5 Plasma discharge of the μ20-III with ion collection by a punching metal. An ion current of 480 mA was obtained at a net microwave power of 100 W and a xenon flow rate of 6 SCCM.

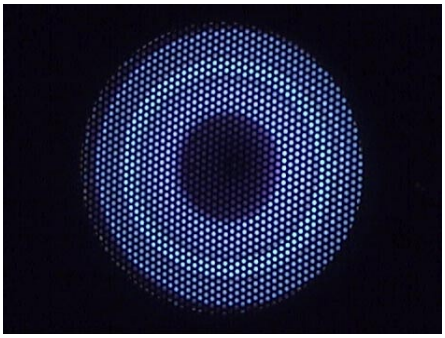

Fig. 6 Plasma discharge of the μ20-IV with ion collection by a punching metal using concentric magnet lines. An ion current of 310 mA was obtained at a microwave power of 120 W (at amplifier output) and a reflected power of 21 W without a triple stub tuner.

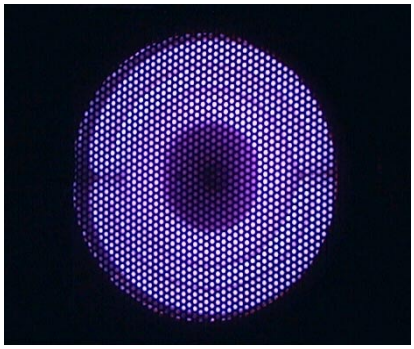

Fig. 7 Plasma discharge of the μ20-IV with ion collection by a punching metal using the same magnet system as shown in Fig. 4-c). An ion current of 420 mA was obtained at a microwave power of 120 W (at amplifier output) and a reflected power of 4 W without a triple stub tuner.

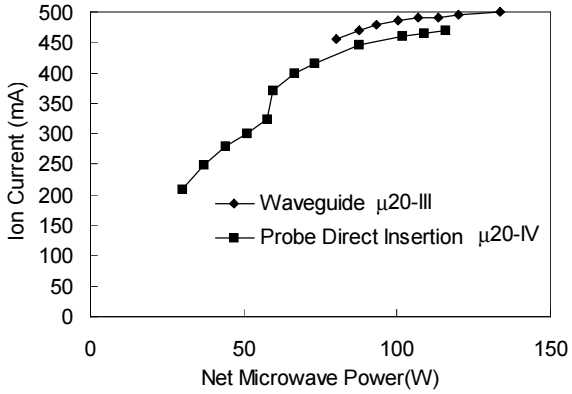

Fig. 8 Ion currents generated using the μ20-IV discharge chamber and collected by a punching metal, as a function of net microwave power compared with the results of the μ20-III.

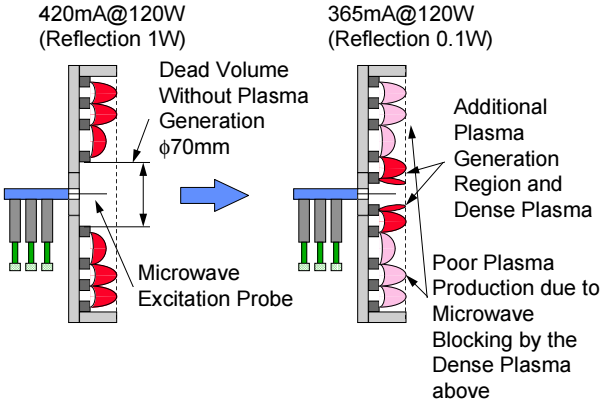

Fig. 9 Negative effect of addition of a magnet ring in the vicinity of the microwave excitation probe.

4. Initial Beam Extraction Test of μ20-III

In order to obtain the correlation between extracted beam currents by using the C/C optics and collected ion current by using a negatively biased punching metal, the initial beam extraction test was carried out by using a tungsten filament as a neutralizer and a main plasma igniter. Grid thicknesses are 0.95 mm for the screen grid 1.0 mm for both the accelerator grid and decelerator grid. Grid separations are 0.45 mm between screen and accelerator and 0.30 mm between accelerator and decelerator, respectively. The axial length of

the discharge chamber was optimized and extended by 2 mm than the punching metal configuration to increase the extracted beam current by 3 %.

Although a detailed performance table has not been made yet, the following outstanding data was obtained: An ion beam current of 530 mA was extracted at a net microwave power of 100 W and a xenon flow rate of 8.9 SCCM. The voltages applied to each grid were 1200 V, -350 V and 0 V, for screen, accelerator and decelerator, respectively. The beam ion production cost was 190 eV/ion and the propellant utilization efficiency was 83 %.

5. Multiple Magnet Lines Type with a Microwave Excitation Probe Covered with a BN Cap (μ20-V)

5.1 Internal Cavity Matching Concept

A triple stub tuner can almost perfectly send back microwaves reflected by the plasma loaded discharge chamber. But if the reflection is too large, a strong standing wave is established between the tuner and the antenna, which may heat up the cable and damage it. Indeed, shortening the cable length between them may reduce the possibility of such malfunctions, but it will become more difficult to arrange the tuner outside the vacuum tank so that the tuner can be operated easily. As for flight model ion engines, tuners should be replaced by the equivalent fixed short-end coaxial lines. To reproduce exactly the same matching capability in such manner is not easy. The best solution is to make the discharge chamber itself matched under the plasma discharge conditions without using an external tuning device. One of such internal cavity impedance matching concepts, which eliminate the standing waves from the microwave transmission line, was first proposed by Asmussen, who introduced a movable sliding short to change the cavity length[13]. The laboratory model of the μ10 and μ20-III followed this concept by using a sliding short at the end of the circular waveguide as shown in Fig. 2, though these should also be replaced by a fixed end for the flight model of the μ20 thruster. A new internal matching methodology was deemed necessary for a post μ20-IV model which does not have a waveguide or a triple-stub tuner.

As shown in Fig. 10, the new type, μ20-V, eliminates the need of a triple-stub tuner by using an antenna covered with a boron nitride (BN) cap and a variable frequency microwave source. The theoretical resonant frequencies and measured resonant frequencies are listed in Table 2 for the μ20-V discharge chamber, with a diameter of 200 mm and an axial length of 20 mm. Reflectometry results conducted by using a vector network analyzer is shown in Fig. 11. The downward peaks indicate resonant modes of the discharge chamber and the peak frequencies were shown in the right hand side column of the Table 2. Some theoretically predicted resonant modes were not clearly observed and there are some resonance-like frequencies found which do not coincide with typical cavity modes but equal to the cutoff frequencies of the circular waveguide with the diameter of 200 mm, even though the physical mechanisms involved are uncertain. Only these discrete frequencies can be used without the triple-stub tuner. All eigenmodes are transverse magnetic (TM) modes and electric field heating of electrons occurs preferably parallel to the central axis. There are neither nodes nor loops along with the axial direction, and thus the resonant frequencies are independent from the axial length. This should ease the tuning with the selected ion optics position, at the final stage of the thruster development.

Table 2 shows that the measured resonant frequency of the TM510 mode is slightly higher than the design value of 4.25 GHz. The chamber diameter should be enlarged so that the resonant frequency decreases in the case without an external tuner.

The actual discharge chamber is not an ideal cylinder with smooth surfaces but a cavity with many projections. This is a cause of the resonant frequency shift from the theoretical values. Also the design frequency may be suddenly changed due to the spacecraft mission requirement to escape interference to the communication subsystem. In that sense, frequency tuning by changing the diameter of the chamber side wall has some impact on, for example , the grid support design.

The μ20-V employs a BN cap as a frequency tuning part by selecting from several pieces with different diameters. The BN cap also protects the root of the antenna from contamination and undesirable multipactor discharge, which may take place between center and outer RF conductors. Installation of a sample BN cap decreased the original resonant frequencies by approximately 20 MHz and improved the resonance quality. BN has a relative dielectric constant of 4.5 and the wavelength inside is smaller than in vacuum. This is equivalent to the situation in a discharge chamber larger in diameter. Thus, we can control the resonant frequency to some extent by changing the BN cap size. In the future implementations, this cap should enable antenna and other microwave feeding components to be isolated from the high voltage of the screen grid, without the need for an external DC block, as illustrated in the right-hand side of Fig. 10. In the development

of larger ion engines, this cap may be used as a grid center support.

Table 2 Eigenmodes in the μ20 discharge chamber.

Mode	Theoretical Resonant Frequency (GHz)	Measured Frequency (GHz)
TM220	4.016	
TM030	4.129	
TM510	4.185	4.272
TM320	4.658	4.620
TM610	4.742	4.752
TM130	4.854	4.851
TM420	5.279	5.280
TM230	5.544	
TM520	5.887	

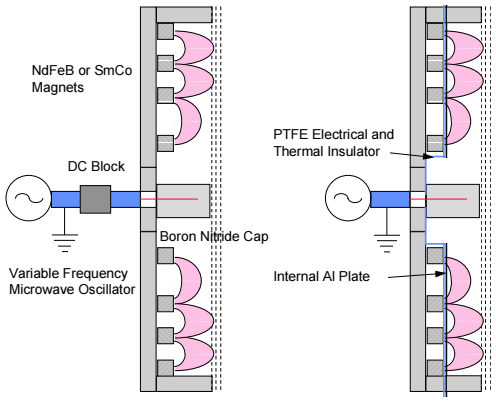

Fig. 10 Schematic diagram of the latest model μ20-V with a BN cap for antenna protection and a variable frequency microwave source. Left hand side : Normal type, Right hand side: With internal electrical insulation capability as a future option.

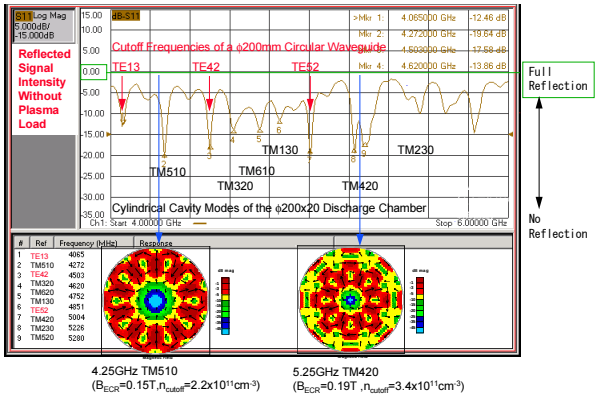

Fig. 11 Microwave resonant characteristics of unloaded μ20-V discharge chamber measured by using a vector network analyzer.

Table 3 An example of the commercially available NdFeB magnet applications at various maximum temperatures.

Maximum Temperature (ºC)	Magnet Model	Residual Induction, B_r (T)
$Nd_2Fe_{14}B$	*HITACHI*	
20	HS-55AH	1.50
60	HS-55AH	1.45
100	HS-55AH	1.38
120	HS-51CH	1.26
140	HS-44CH	1.20
180	HS-47DH	1.12
200	HS-43EH	1.02
Sm_2Co_{17}	*NEC/TOKIN*	
20	LM-30F	1.10
200	LM-30F	1.03

5.2 Application of NdFeB Magnets for Performance Improvement

The magnetic field inside the μ20 is important for both plasma production and plasma confinement, so as to suppress wall loss. For a given microwave frequency, the stronger the flux density at the magnet surface is, the higher the performance, due to the increase in the mirror ratio. As for the μ20, a 10 % increase in magnetic flux density will move the equipotential lines by 1 mm far away from the magnet surface. This will decrease the ion production cost by decreasing the ion loss fraction.

Bucket type ECR plasma sources, such as the μ10 and μ20, cannot produce overdense plasma in which the electron density exceeds the critical value, so called cutoff density, determined by the microwave frequency. The cutoff density is proportional to the square of the frequency, in other words, the ECR magnetic field strength. Combination of stronger magnetic field and higher microwave frequency will increase the thrust density in theory. For example, a 10 % higher frequency may increase the thrust density by 21 %.

The ion production costs at higher microwave powers are larger than at lower powers as shown in Fig. 8. This is probably because the coupling efficiency between the microwave and the plasma deteriorates as the plasma density reaches the cutoff-density threshold, resulting in and increase in microwave reflections inside the discharge chamber. Consequently, operation at plasma density levels slightly lower than the cutoff density is preferable in order to achieve lower ion production costs. For the reasons stated above, the adoption of stronger magnets and/or higher microwave frequencies is a very attractive and interesting approach from a performance point of view.

For many years, ring-cusp ion thrusters and the μ10 have employed SmCo magnets. It is safe to say that

this magnet production technology is well-matured and stronger SmCo magnet types are not expected to be developed in the future. On the other hand, NdFeB magnets have been steadily improved in both residual induction and coercive force, and there are many stronger types available in the market that can be employed under higher temperature conditions at the present time, in comparison with the same technology back five years ago.

Table 3 summarizes an example of magnet selection depending on the maximum operating temperatures according to a manufacturer's catalog. It is clear that the lower the operating temperature is, the stronger the available magnets are. NdFeB magnets are advantageous to the SmCo magnets at temperature range below 200 ºC. A NdFeB magnet HS-44CH with a maximum energy product of 44 MOe was selected in the first trial for the application to the μ20. This magnet can tolerate temperatures of 140 ºC and so far no degradation was found during 1 hour continuous operation without special thruster cooling.

5.3 Microwave Frequency Tracking for Perfect Impedance Matching

As for μ20-V, the plasma discharge can be initiated simultaneously with the microwave insertion at frequencies listed in Table 2 and the required power for ignition is less than 30 W due to the microwave resonance inside the cavity. After plasma ignition, the reflected power is greater than the one before ignition, due to the shift of the resonant frequency with plasma load presence. Microwave power and gas pressure also affects the microwave impedance matching. Because μ20-V does not have any moving parts, optimization of the impedance matching was attempted by changing the oscillator frequency. The employed microwave signal generator has an accuracy of 100 kHz. Although there were a few cases in which reflected power reached 5-10 W and could not be suppressed perfectly, almost always the reflected power was less than 1 % of the forward power, which corresponds to a voltage standing wave ratio (VSWR) of less than 1.22. The largest ion current so far was updated by this method with the TM420 mode at a frequency of 5.27 GHz by using NdFeB magnets only. Fig. 12 shows the beam current, the reflected microwave power and the microwave frequency as a function of the net microwave power. Ion currents were collected by a punching metal grid and translated into the expected beam currents by using the correlation taken in the μ20-III beam extraction experiment as described in the section 4. The optimum frequency for the plasma ignition was 5.2260 GHz and the one for the maximum microwave power input was 5.2937 GHz. A frequency variation of 70 MHz was sufficient to maintain perfect matching condition under the wide range of microwave power. Because traveling wave tube (TWT) amplifiers have a bandwidth of 300 MHz, only a variable frequency oscillator for space applications needs to be developed, which should not pose major technically difficulties by using direct signal synthesizer (DSS) technology.

5.4 Effects of Microwave Frequency and Magnetic Field Strength on Performance

The performance of the μ20-V with NdFeB magnets and μ20-V with SmCo magnets was compared at various frequencies ranging from 4 to 6 GHz as shown in Fig. 13. The μ20-V with NdFeB magnets could not be operated at frequencies higher than 5.8 GHz due to abrupt plasma extinction. The μ20-V with SmCo magnets could not be operated at frequencies higher than 5.5 GHz due to the same reason. The optimum frequencies to generate largest currents are 5 GHz and 5.27 GHz for SmCo and NdFeB magnets, respectively. At relatively smaller microwave powers, lower frequency shows better performance with the same magnetic field because of the better plasma confinement achieved by the larger mirror ratio. On the other hand, at larger microwave powers, the higher the frequency, the larger the obtained ion current. This is due to the cutoff density increase. At the middle power range, between 45 and 80 W, SmCo magnets were superior to the NdFeB magnets probably due to dense plasma generation over the innermost magnet ring, which prevents microwave transmission to the outer region in the discharge chamber. Fig. 13 suggests that there is an optimum combination of the frequency and the magnet type depending on the required thrust density.

It should be noted that the μ20-V performance was not improved at the original target frequency of 4.25 GHz, as compared with μ20-III and μ20-IV. This is because the plasma confinement by the SmCo magnets was sufficiently good. We have to stick to this frequency because this is the highest frequency at which space qualified C-band TWT amplifiers are available as transmitters for spacecraft communication. In order to increase beam current at 4.25 GHz, completely different modification to the discharge chamber will be necessary. As the first step, the resonant frequency of the TM510 mode with plasma load, which now largely shifts to 4.5GHz after plasma ignition, should be well-tuned to the target frequency of 4.25 GHz by proper enlarging of the BN cap diameter.

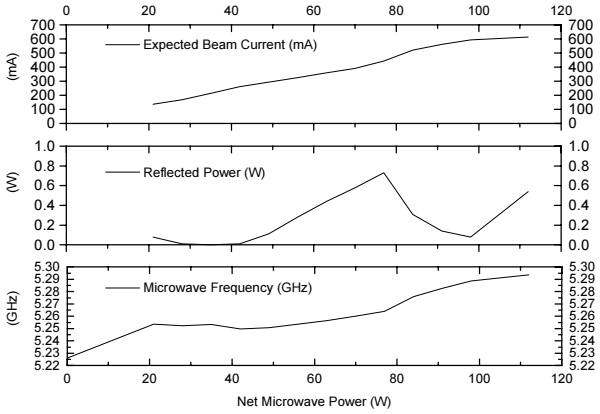

Fig. 12 Demonstration of frequency tracking to maintain the perfect impedance matching condition in the TM420 cylindrical cavity mode.

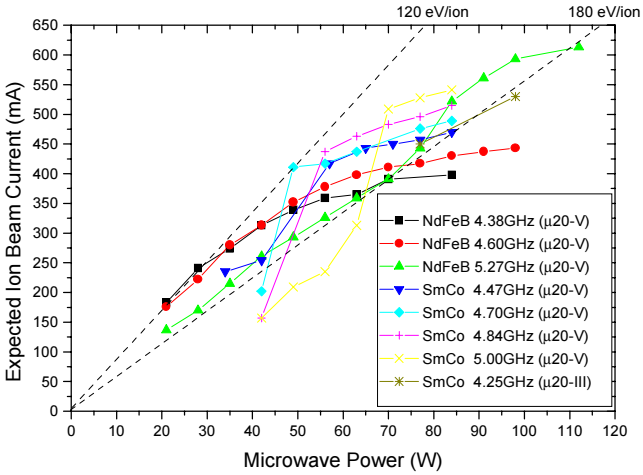

Fig. 13 Effects of microwave frequency and magnetic field strength on performance.

6. Conclusion

A 30-mN class microwave discharge ion thruster has been under development and steadily improvements in thrust density and ion production cost have been obtained. The latest prototype, μ20-V, which has a compact microwave launcher covered with a BN cap for antenna protection and impedance matching, will generate at least 30 mN of thrust with an ion production cost of less than 190 eV. Employment of higher frequencies and stronger NdFeB magnets has turned out to be very promising for thrust density increase and ion production cost decrease, although the need for new TWT amplifiers, developed specifically for microwave ion engine applications, may result in prohibitive costs for total system implementation. Further improvements will be continued in order to increase the ion beam current at the frequency of 4.25 GHz.

References

[1] Toki, K., Kuninaka, H., Nishiyama, K. and Shimizu, Y., "Flight Readiness of the Microwave Ion Engine System for MUSES-C Mission," IEPC Paper 2003-98, Mar 2003.
[2] Kuninaka, H., "Orbit toward Jupiter by Electric Propelled Delta-V Earth Gravity Assist," ISTS Paper 2002-b-08, May 2002.
[3] Ozaki, T., Gotoh, Y., Itoh, T. and Kajiwara, K., "Development Status of 20 mN Class Xenon Ion Thruster for ETS-8," IEPC Paper 01-102, October 2001.
[4] Kitamura, S., Hayakawa, Y., Miyazaki, K., Kajiwara, K., Yoshida, H., Yamamoto, Y. and Akai, K., "Results of a 35-cm Xenon Ion Thruster Endurance Test," IEPC Paper 01-083, October 2001.
[5] Funaki, I., Nishiyama, K., Kuninaka, H., Toki, K., Shimizu, Y. and Toki, H., "20mN-class Microwave Discharge Ion Thruster," IEPC Paper 01-103, October 2001.
[6] Shimizu, Y., Kuninaka, Nishiyama, K. and Toki, K., "Evaluation of New Carbon-Carbon Composite Material for a 20 cm Ion Engine," IEPC Paper 2003-97, Mar 2003.
[7] Goede, H., "30-cm Electron Cyclotron Plasma Generator," Journal of Spacecraft, Vol.24 No. 5, pp.437-443, September-October 1987.
[8] Miyoshi, H., Ichimura, S., Kuninaka, H., Kuriki, K., Horiuchi, Y., "Microwave Ion Thruster with Electron Cyclotron Resonance Discharge," IEPC Paper 91-084, October 1991.
[9] Kuninaka, H., Hiroe, N., Kitaoka, K., Ishikawa, Y, Nishiyama, K and Horiuchi, Y., "Development of Ion Thruster System for Interplanetary Missions," IEPC Paper 93-198, September 1993.
[10] Geisler, M., Kieser, J. and Wilhelm, R., "Elongated microwave electron cyclotron resonance heating plasma source," Journal of Vacuum and Science Technology A, Vol. 8, No.2, pp.908-915, March-April 1990.
[11] Funaki, I., et al., "Verification Tests of 10-cm-diam. Carbon-Carbon Composite Grids for Microwave Discharge Ion Thruster," IEPC Paper 99-164, October 1999.
[12] Toki, H., Fujita, H., Nishiyama, K., Kuninaka, H., Toki, K. and Funaki, I., "Performance Test of Various Discharge Chamber Configurations for ECR Discharge Ion Thruster," IEPC Paper 01-107, October 2001.
[13] Asmussen, J. and Mak, P., "Control of Multipolar Electron Cyclotron Resonance Discharges using Internal Cavity Impedance Matching," Rev. Sci. Instrum., Vol. 65, No. 5, May 1994.